View metadata, citation and similar papers at core.ac.uk

brought to you by CORE

provided by Copenhagen University Research Information System

UNIVERSITY OF COPENHAGEN

Temporal dynamics of avian populations during pleistocene revealed by whole-genome sequences

Nadachowska-Brzyska, Krystyna; Li, Cai; Smeds, Linnea; Zhang, Guojie; Ellegren, Hans

Published in:
Current Biology

DOI:
10.1016/j.cub.2015.03.047

Publication date:
2015

Document version
Publisher's PDF, also known as Version of record

Document license:
CC BY-NC-ND

Citation for published version (APA):
Nadachowska-Brzyska, K., Li, C., Smeds, L., Zhang, G., & Ellegren, H. (2015). Temporal dynamics of avian populations during pleistocene revealed by whole-genome sequences. *Current Biology*, *25*(10), 1375-1380. https://doi.org/10.1016/j.cub.2015.03.047

Download date: 08. Apr. 2020

Report

Current Biology

Temporal Dynamics of Avian Populations during Pleistocene Revealed by Whole-Genome Sequences

Highlights

- Cyclic N_e changes have been a common feature of many birds during the Quaternary period
- Severe reductions in N_e coincide with the beginning of the last glacial period
- Species with long-term decline in N_e may be especially vulnerable to recent threats

Authors

Krystyna Nadachowska-Brzyska, Cai Li, ..., Guojie Zhang, Hans Ellegren

Correspondence

krystyna.nadachowska-brzyska@ebc.uu.se

In Brief

The abundance and distribution of life on Earth has been critically influenced by global climatic oscillations. Nadachowska-Brzyska et al. show that many bird species experienced cycles of population contractions and expansion during the Quaternary period, and that severe declines in effective population size often coincided with the beginning of the last glacial period.

Nadachowska-Brzyska et al., 2015, Current Biology *25*, 1375–1380
May 18, 2015 ©2015 The Authors
http://dx.doi.org/10.1016/j.cub.2015.03.047

Current Biology
Report

Temporal Dynamics of Avian Populations during Pleistocene Revealed by Whole-Genome Sequences

Krystyna Nadachowska-Brzyska,[1,*] Cai Li,[2,3] Linnea Smeds,[1] Guojie Zhang,[2,4] and Hans Ellegren[1]
[1]Department of Evolutionary Biology, Evolutionary Biology Centre, Uppsala University, Norbyvägen 18D, 752 36 Uppsala, Sweden
[2]China National GeneBank, BGI-Shenzhen, Shenzhen 518083, China
[3]Centre for GeoGenetics, Natural History Museum of Denmark, University of Copenhagen, Øster Voldgade 5-7, 1350 Copenhagen, Denmark
[4]Centre for Social Evolution, Department of Biology, Universitetsparken 15, University of Copenhagen, 2100 Copenhagen, Denmark
*Correspondence: krystyna.nadachowska-brzyska@ebc.uu.se
http://dx.doi.org/10.1016/j.cub.2015.03.047
This is an open access article under the CC BY-NC-ND license (http://creativecommons.org/licenses/by-nc-nd/4.0/).

SUMMARY

Global climate fluctuations have significantly influenced the distribution and abundance of biodiversity [1]. During unfavorable glacial periods, many species experienced range contraction and fragmentation, expanding again during interglacials [2–4]. An understanding of the evolutionary consequences of both historical and ongoing climate changes requires knowledge of the temporal dynamics of population numbers during such climate cycles. Variation in abundance should have left clear signatures in the patterns of intraspecific genetic variation in extant species, from which historical effective population sizes (N_e) can be estimated [3]. We analyzed whole-genome sequences of 38 avian species in a pairwise sequentially Markovian coalescent (PSMC, [5]) framework to quantitatively reveal changes in N_e from approximately 10 million to 10 thousand years ago. Significant fluctuations in N_e over time were evident for most species. The most pronounced pattern observed in many species was a severe reduction in N_e coinciding with the beginning of the last glacial period (LGP). Among species, N_e varied by at least three orders of magnitude, exceeding 1 million in the most abundant species. Several species on the IUCN Red List of Threatened Species showed long-term reduction in population size, predating recent declines. We conclude that cycles of population expansions and contractions have been a common feature of many bird species during the Quaternary period, likely coinciding with climate cycles. Population size reduction should have increased the risk of extinction but may also have promoted speciation. Species that have experienced long-term declines may be especially vulnerable to recent anthropogenic threats.

RESULTS AND DISCUSSION

Effective Population Sizes of Birds during the Quaternary Period

We had data of sufficient resolution to estimate historical effective population sizes (N_e) using the pairwise sequentially Markovian coalescent (PSMC) approach for 38 bird species (Table S1) over a range from 1–10 million years ago (Mya) up until about 10 thousand years ago (kya). This implied that we could follow population trends at the beginning of, and in many cases during, the last glacial period (LGP, 110–12 kya; Figures 1, 2, 3, 4, and S1). There was considerable variability in N_e among species as indicated by the mean value over time, ranging from 30,000–40,000 in rhinoceros hornbill, bald eagle, and kea to approximately 1,500,000–2,700,000 in budgerigar, killdeer, and domestic pigeon. Similarly, the maximum N_e estimated over the time span analyzed varied between 60,000–70,000 (e.g., kea and Dalmatian pelican) and >4,000,000 (domestic pigeon, killdeer, and budgerigar), and the minimum N_e between 1,000–3,000 (e.g., rhinoceros hornbill and white-tailed eagle) and 400,000–550,000 (common cuckoo, little egret, and red-legged seriema). This illustrates that N_e varied by at least three orders of magnitude among bird species during the Quaternary period.

The studied species cover the full spectrum of avian diversity, representing all orders of extant birds. We found no phylogenetic signal in the distribution of N_e estimates (Abouheif test, $p > 0.1$ for all tests). This may be because most internodes in a phylogenetic tree of these species are short, reflecting rapid radiation of most avian orders soon after the Cretaceous-Paleogene boundary [6].

Cycles of Population Expansions and Contractions

An immediate observation when analyzing individual species is that N_e has in most cases varied considerably over time. Cycles of population expansions and contractions have thus been a common feature of many birds during the Quaternary period, and this seems independent of the overall abundance of a particular species. As an example, the downy woodpecker (Figure 1) had a moderate N_e of approximately 150,000 at 2 Mya but then reached 1,200,000 after two periods of demographic expansion separated by an episode of small contraction. However, a severe decline around 100 kya decreased N_e from over

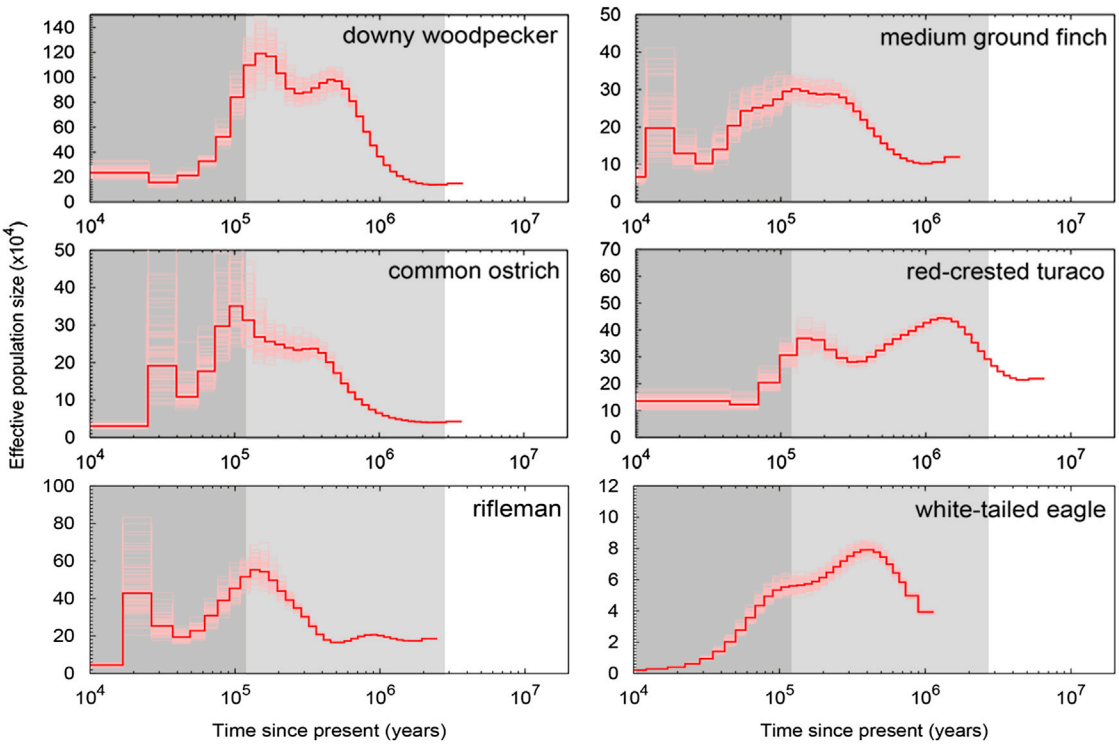

Figure 1. Drastic Decline of Effective Population Size at the Beginning of the Last Glacial Period

The plots represent examples of species where PSMC analysis reveals clear signs of severe reduction in N_e coinciding with the beginning of the LGP. The red curve is the PSMC estimate for the original data; the pink curves indicate PSMC estimates for 100 bootstrapped sequences. The gray shaded areas indicate the Pleistocene period, with the LGP shown in darker gray. Note that in this and all subsequent figures, most recent data are at left on the x axis, with data running further into the past as one travels rightward. See also Table S1, Figure S1, and Figure S3.

1,000,000 to 200,000. As another example, the barn owl also experienced two cycles of population expansion and contraction (Figure 2). The second decline, around 160 kya, decreased N_e to 30,000 individuals. Other examples of complex N_e dynamics with alternating periods of decline and increase are presented in Figures 1, 2, 3, 4, and S1.

We suggest that a common pattern of multiple cycles of population decline and increase, most occurring <1 Mya, are a direct consequence of repeated and drastic changes in the global climate over the last few million years. During the Pleistocene, climatic glaciation dynamics changed from 41,000-year cycles to 100,000-year cycles approximately 0.9 Mya and became increasingly dramatic [7]. As a consequence, habitat distributions changed and species had to retract to glacial refugia or adopt to new environmental conditions during glacial maxima [2, 3]. Such events are likely to have been associated with more or less severe reductions in population size, with potential for recovery during mild periods.

The single most common pattern in our data is the severe reduction in population size approximately coinciding with the beginning of the LGP or occurring during this period (Figure 1). This was observed in 22 of the 38 studied species (58%) and included species from all parts of the world. For example, both eagle species declined from approximately 60,000 individuals right before the LGP to only a few thousand (2,000 and 6,000) by the end of the LGP. The ostrich experienced a dramatic 10-fold decline from approximately 350,000 individuals to 30,000 individuals during the same time period.

A clear and drastic reduction in N_e at the beginning of or during the LGP was not observed for all species. This may be due to the fact that, for some species, the resolution of the PSMC analysis in recent times (including LGP) was poor (Figure S1), or simply that some species were less affected by the last glaciation than others (Figures 3 and S1). We tested the hypothesis that species with current ranges that overlap areas previously covered by ice sheets or other extreme environments (such as extreme deserts) might show more severe population reductions as compared to species occurring in less variable conditions [2, 3]. To do this, we divided the data into species with a current range overlapping areas that were previously covered by extreme environments versus species with no such overlap (similar to [8]; Table S1). We then calculated a decline metric during the LGP as $1 - (N_{recent}/N_{110\ kya})$, but we found no correlation between the present distribution of species and severity of decline (Mann-Whitney test, $p = 0.37$). This could be for several reasons, including both large variances in the most recent PSMC estimates and an oversimplified categorization of species with respect to sensitivity to climate change.

The role of Pleistocene speciation and extinction events in avian diversification has been a matter of long-standing debate [9]. Some studies have reported high speciation rates during the Pleistocene epoch [8, 10], while others have argued that

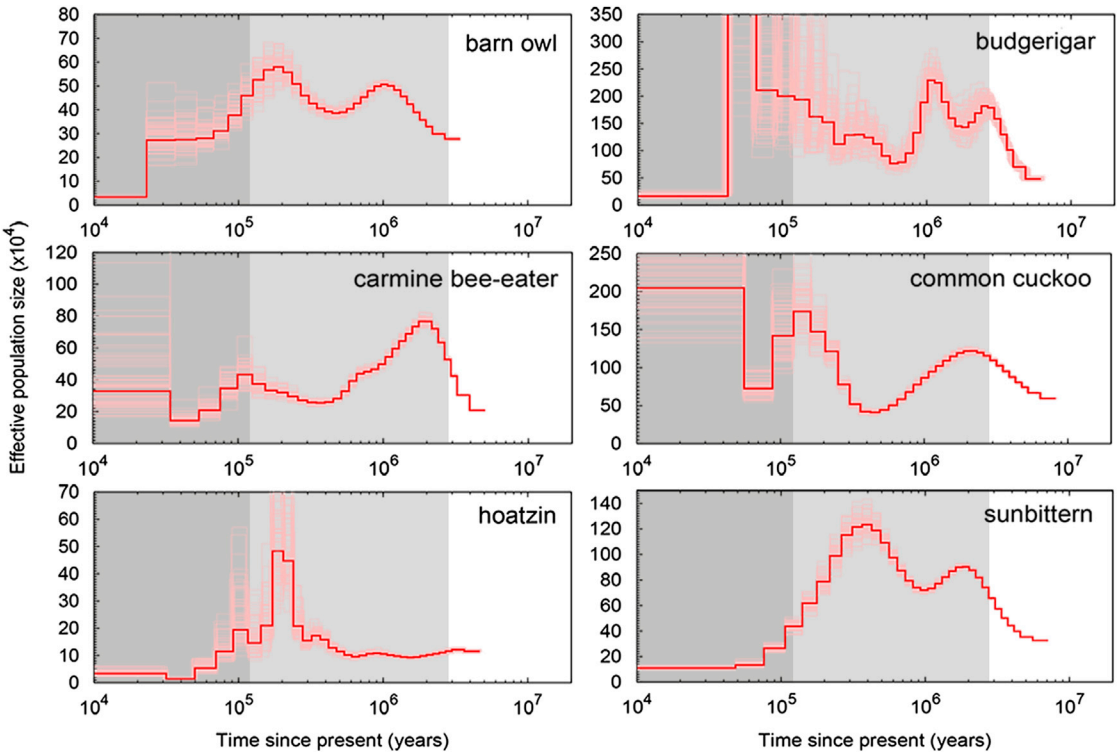

Figure 2. Cycles of Population Expansions and Contractions

Examples of PSMC estimates of changes in the effective population size change over time, representing variation in inferred N_e dynamics. The red curve is the PSMC estimate for the original data; the pink curves indicate PSMC estimates for 100 bootstrapped sequences. The gray shaded areas indicate the Pleistocene period, with the LGP shown in darker gray. See also Table S1, Figure S1, and Figure S3.

the tempo of diversification slowed down during that period due to either lowered speciation rate or increased extinction rate [11, 12]. The fossil record suggests that many species experienced significant range shifts during increasingly dramatic Pleistocene glaciation events [4]. Our results document significant population size changes during this time, including strong reductions in N_e, especially during the LGP. This may have led to increased extinction rates, as low N_e can lead to inbreeding depression and accumulation of deleterious mutations as well as limited ability to adapt to changing environments due to reduced genetic variation [13]. However, lowered N_e may have promoted population structure and, coupled with refugial isolation, diversification and ultimately speciation. In this context, it is worth noting that for many of the lineages for which we derived N_e estimates over time, one or more speciation events are likely to have occurred during this period.

Population Trends of Threatened Species

Six of the species in our study are classified as endangered (EN, two species) or vulnerable (VU, four species) on the IUCN Red List of Threatened Species (http://www.iucnredlist.org/), and another two as near threatened (NT). Population trends of these species varied (Figure 3). Both species classified as endangered experienced long-term decrease in N_e, from respectively 100,000 (crested ibis) and 250,000 (gray crowned crane) at 0.5–1 Mya to 30,000–40,000 individuals at 20–40 kya, and in the case of the crested ibis probably down to the level of 2,000 individuals at 10 kya.

Two species listed as vulnerable (brown mesite and kea) showed clear signs of population decline, whereas two others seem to have had rather stable N_e during the LGP (MacQueen's bustard and the Dalmatian pelican). The brown mesite had high N_e (200,000–350,000) for a long time until approximately 30 kya, when it faced a drastic decline to 23,000. The kea had relatively low but constant N_e (40,000) throughout its evolutionary history but experienced a drastic reduction in N_e to 4,000 individuals just within the last 20,000 years of the LGP. The Dalmatian pelican also experienced a 2-fold decline in N_e from 200 kya and was then stable toward the end of LGP. The rhinoceros hornbill (NT; Figure 4) experienced an extreme and continuous decline from 70,000 individuals approximately 1 Mya to less than 2,000 individuals 10 kya.

Although most species on the IUCN Red List probably have experienced very recent and severe declines, it is important to note that our data demonstrate that many of them have also been subject to more long-term population reductions. This suggests that species that already have relatively low N_e might be particularly vulnerable to extinction following anthropogenic interference.

Recent and drastic bottlenecks, and associated severe inbreeding, can lower PSMC-based N_e estimates in recent times and erase information about ancient N_e dynamics. To test whether recent population size changes in endangered species

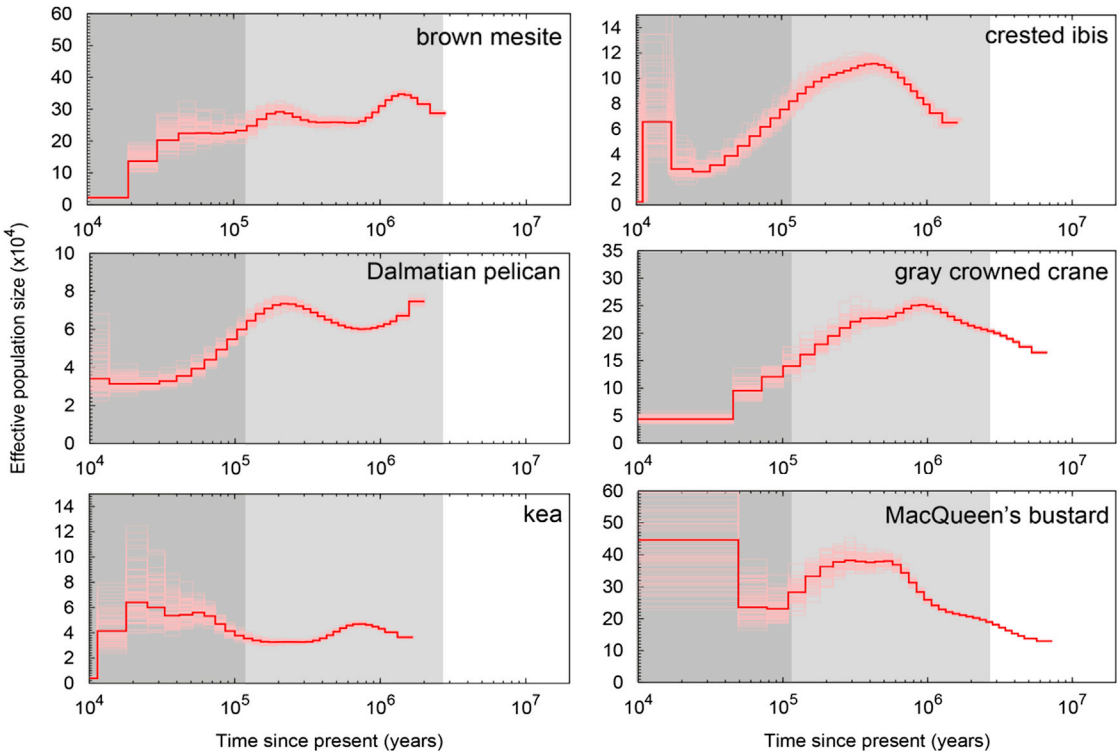

Figure 3. Temporal Dynamics of Effective Population Size for Species Indicated as Threatened on IUCN Red List of Threatened Species
The red curve is the PSMC estimate for the original data; the pink curves indicate PSMC estimates for 100 bootstrapped sequences. The gray shaded areas indicate the Pleistocene period, with the LGP shown in darker gray. See also Table S1 and Figures S1–S3.

affected inference of ancestral N_e dynamics, we identified and masked as missing data long runs of homozygosity (RoH). The estimated N_e trajectories were not affected by the removal of the RoH regions (Figure S2), indicating that sufficiently divergent segments were present in the analyzed genomes and that inference about N_e dynamics over time was still possible. On a related note, we similarly masked RoH regions in the genomes of the two domestic species, Pekin duck and domestic pigeon, which might have experienced inbreeding during domestication. As in the case of IUCN Red List species, estimated N_e trajectories were not affected by the removal of the RoH regions in these species (Figure S2).

A set of species relevant from a conservation perspective includes those that are not currently categorized as Threatened or Near Threatened by IUCN but that show evidence of long-term decrease in N_e (Figure 4). For example, N_e of the white-tailed tropicbird has been declining since 1 Mya to reach a level of only 1,000 individuals 10 kya, and the turkey vulture (buzzard) experienced a long-term decline reaching an N_e of 20,000 individuals in the last part of the LGP (50 kya; Figure 4). These species may be considered as potentially vulnerable due to low levels of genetic diversity in the relatively recent past.

Finally, we investigated the N_e/N ratio, where N is census size and N_e was taken from the most recent estimate in the PSMC analysis (Table S1). In contemporary populations, the N_e/N ratio may be on the order of 0.1 [13], but significant deviations from this can potentially be expected for species that have very recently experienced severe declines ($N_e/N > 0.1$) or expansions ($N_e/N < 0.1$). In accordance with this, all species with an N_e/N ratio higher than 0.75 are on the IUCN Red List, indicating recent and severe population contractions. On the other end of the distribution, species with an N_e/N of 0.01 or less include pigeon, mallard, and barn owl, cosmopolitan species that are very common.

Methodological Issues

PSMC is a powerful method to infer changes in N_e over time, but it is also associated with several sources of uncertainty, which are important to consider. Mutation rate and generation time estimates are necessary to scale the results of the PSMC analysis. If these estimates are under- or overestimated, the PSMC would also be biased. However, mutation rate and generation time estimates influence the PSMC plots in a predictable manner. They do not change the shape of the PSMC curve but only move the curve along the axes (Figure S3). For example, a halved generation time will double the estimate of N_e (given a fixed mutation rate per year), and a halved mutation rate per year will move the curve backward in time and also double the estimate of N_e.

Conclusions

The abundance and distribution of life on Earth has been critically influenced by global climatic oscillations. Importantly, the last few million years have been characterized by increasingly dramatic glaciation [1]. Revealing the temporal dynamics of N_e during such periods is critically important if we are to fully

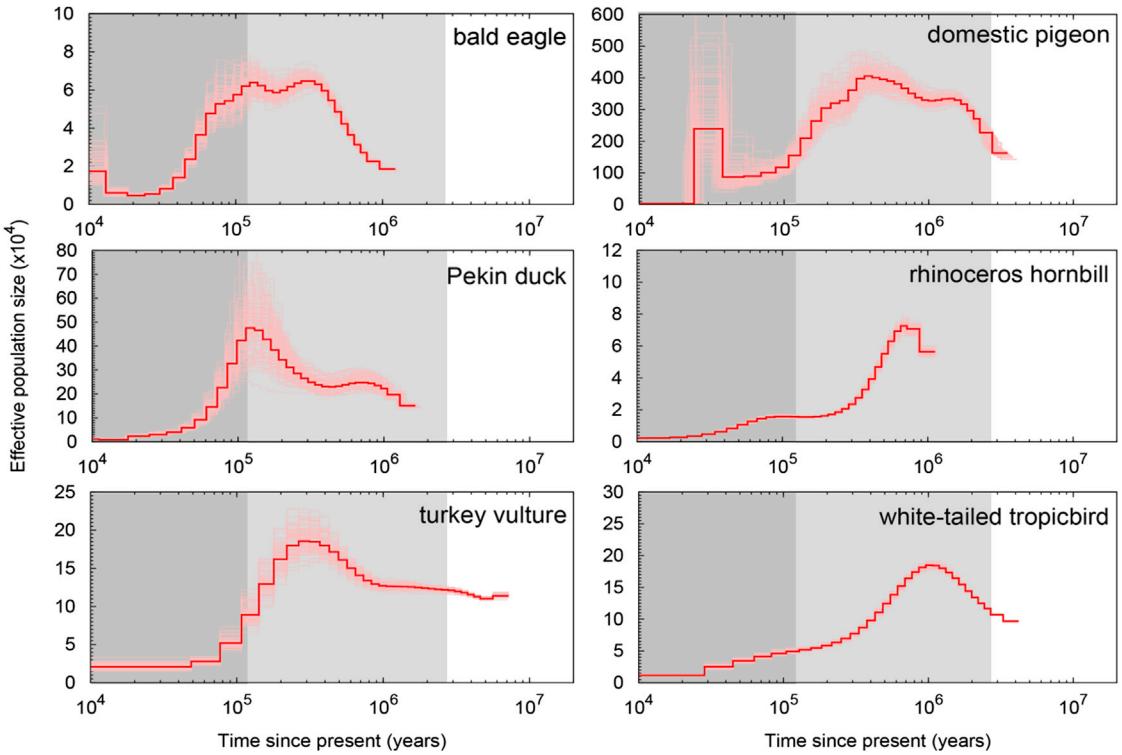

Figure 4. Long-Term Decrease in Effective Population Size

The plots represent examples of species with persistent declines in N_e that are not indicated as Threatened on the IUCN Red List of Threatened Species. The red curve is the PSMC estimate for the original data; the pink curves indicate PSMC estimates for 100 bootstrapped sequences. The gray shaded areas indicate the Pleistocene period, with the LGP shown in darker gray. See also Table S1, Figure S1, and Figure S3.

understand the evolutionary consequences of global climate changes as well as recent anthropogenic impact on climate and biodiversity [14]. However, up until recently, coalescent modeling of different demographic scenarios has failed to infer ancestral population size and explicitly model changes in N_e over time.

PSMC analysis offers a unique means to reveal changes in N_e over time and can therefore deepen our understanding of species dynamics driven by climate change. Here we have shown that N_e dynamics in many species of birds have been characterized by cycles of population expansion and contraction during the Quaternary period, likely coinciding with climate cycles. In particular, many species experienced a drastic reduction in population size at the beginning of the LGP. Coupled with more recent anthropogenic threats, this may impact both evolvability and the long-term survival capacity of extant bird lineages.

Current biodiversity patterns of birds (almost 10,500 extant species distributed across 37 orders [15]) have been shaped by several macroecological and macroevolutionary processes including past climate dynamics, rapid radiations, and increase in diversification rate over the last 50 million years [16, 17]. More recently, Quaternary climate fluctuations and destruction of natural habitats through human activities have impacted the distribution and abundance of avian diversity [4, 18]. The results from our study document that such climate events significantly affect the effective breeding sizes of bird populations.

EXPERIMENTAL PROCEDURES

We analyzed 38 bird species that have been genome sequenced using similar sequencing and assembly methodologies as reported recently [6, 19] (Table S1). All analyzed genomes had mean coverage $\geq$ 24× (Table S1), enabling proper estimation of genotype states for most of the sites [20, 21]. For each species, we obtained a diploid consensus genome sequence and filtered it by excluding sites at which the root-mean-square mapping quality of reads covering the site was below 25, the inferred consensus quality was below 20, and read depth was either more than twice or less than one-third of the average read depth across the genome. These filters removed 7% of sites on average and were applied to minimize the impact of incorrectly called genotypes (e.g., false heterozygote sites) in the data. Filtered genome sequences were used in PSMC analysis [5].

To decide which PSMC settings would be most appropriate for each species, we ran several pilot runs with different combinations of three PSMC arguments: number of free atomic time intervals (–p option), upper limit of time to most recent common ancestor (TMRCA) (–t option), and initial value of $r = \theta/\rho$ (–r option). The values were chosen according to our previous experience [22] and suggestions by H. Li and R. Durbin (https://github.com/lh3/psmc). Pilot runs of PSMC indicated that the number of free atomic intervals and the upper limit of TMRCA had little influence on the shape of the PSMC curves and that convergence was obtained faster with r = 5 than with r = 1. Based on the results from the pilot runs, we chose the final settings for the PSMC to be "N30 –t5 –r5 –p 4+30*2+4+6+10" for all species. To determine variance in N_e estimates, we performed 100 bootstraps for each species.

We scaled results to real time using estimates of generation time and mutation rate. We used branch-specific estimates of the synonymous substitution rate per synonymous site (d_S) from a dated phylogeny based on a phylogenomic analysis of the genomes studied herein [6] as proxies for rate of mutation [23]. This meant that each species could be assigned a unique d_S estimate.

Information on generation times for birds is limited. We therefore used age of sexual maturity multiplied by a factor of two as a proxy for generation time. This transformation has proved applicable to other avian systems where detailed information on age-specific rates of survival and reproductive output, necessary for estimating generation time, has been obtained [24]. Information on the age of sexual maturity was obtained from the literature (Table S1). The minimum, maximum, and average N_e over time were calculated using approximated mutation (μ) rate and the equation given by H. Li and R. Durbin (https://github.com/lh3/psmc, $N_e = N_0 * \lambda_k$, where N_0 and λ_k are estimated by the PSMC model). To test for a phylogenetic signal in N_e estimates, we used Abouheif's C_{mean} statistic and 1,000 permutation tests [25].

SUPPLEMENTAL INFORMATION

Supplemental Information includes three figures and one table and can be found with this article online at http://dx.doi.org/10.1016/j.cub.2015.03.047.

AUTHOR CONTRIBUTIONS

K.N.-B. and H.E. conceived and designed the experiments. K.N.-B. analyzed the data. C.L., G.Z., and L.S. provided data or scripts. K.N.-B. and H.E. wrote the manuscript.

ACKNOWLEDGMENTS

We thank Reto Burri for assistance with figures and two anonymous reviewers for helpful comments. Financial support was obtained via an Advanced Investigator Grant (NEXTGENMOLECOL) from the European Research Council, a Wallenberg Scholar Award from the Knut and Alice Wallenberg Foundation, and the Swedish Research Council (2007-8731, 2010-5650, and 2013-8271), all to H.E. Computations were performed on resources provided by the Swedish National Infrastructure for Computing (SNIC) through the Uppsala Multidisciplinary Center for Advanced Computational Science (UPPMAX).

Received: December 22, 2014
Revised: March 6, 2015
Accepted: March 23, 2015
Published: April 16, 2015

REFERENCES

1. Williams, D., Dunkerly, D., DeDeckker, P., Kershaw, P., and Chappell, M. (1988). Quaternary Environments. (Arnold).
2. Hewitt, G. (2000). The genetic legacy of the Quaternary ice ages. Nature *405*, 907–913.
3. Hewitt, G.M. (2004). Genetic consequences of climatic oscillations in the Quaternary. Philos. Trans. R. Soc. Lond. B Biol. Sci. *359*, 183–195, discussion 195.
4. Holm, S.R., and Svenning, J.-C. (2014). 180,000 years of climate change in Europe: avifaunal responses and vegetation implications. PLoS ONE *9*, e94021.
5. Li, H., and Durbin, R. (2011). Inference of human population history from individual whole-genome sequences. Nature *475*, 493–496.
6. Jarvis, E.D., Mirarab, S., Aberer, A.J., Li, B., Houde, P., Li, C., Ho, S.Y.W., Faircloth, B.C., Nabholz, B., Howard, J.T., *et al*. (2014). Whole-genome analyses resolve early branches in the tree of life of modern birds. Science *346*, 1320–1331.
7. Rahmstorf, S. (2002). Ocean circulation and climate during the past 120,000 years. Nature *419*, 207–214.
8. Weir, J.T., and Schluter, D. (2004). Ice sheets promote speciation in boreal birds. Proc. Biol. Sci. *271*, 1881–1887.
9. Lovette, I.J. (2005). Glacial cycles and the tempo of avian speciation. Trends Ecol. Evol. *20*, 57–59.
10. Johnson, N.K., and Cicero, C. (2004). New mitochondrial DNA data affirm the importance of Pleistocene speciation in North American birds. Evolution *58*, 1122–1130.
11. Klicka, J., and Zink, R.M. (1997). The importance of recent ice ages in speciation: a failed paradigm. Science *277*, 1666–1669.
12. Zink, R.M., Klicka, J., and Barber, B.R. (2004). The tempo of avian diversification during the Quaternary. Philos. Trans. R. Soc. Lond. B Biol. Sci. *359*, 215–219, discussion 219–220.
13. Frankham, R. (1995). Conservation genetics. Annu. Rev. Genet. *29*, 305–327.
14. Pauls, S.U., Nowak, C., Bálint, M., and Pfenninger, M. (2013). The impact of global climate change on genetic diversity within populations and species. Mol. Ecol. *22*, 925–946.
15. Dickinson, E., and Remsen, J. (2013). The Howard and Moore Complete Checklist of the Birds of the World. (Aves Press).
16. Jetz, W., Thomas, G.H., Joy, J.B., Hartmann, K., and Mooers, A.O. (2012). The global diversity of birds in space and time. Nature *491*, 444–448.
17. Jarvis, E.D., Mirarab, S., Aberer, A.J., Li, B., Houde, P., Li, C., Ho, S.Y., Faircloth, B.C., Nabholz, B., Howard, J.T., *et al*.; Avian Phylogenomics Consortium (2015). Phylogenomic analyses data of the avian phylogenomics project. Gigascience *4*, 4.
18. Gaston, K.J., Blackburn, T.M., and Klein Goldewijk, K. (2003). Habitat conversion and global avian biodiversity loss. Proc. Biol. Sci. *270*, 1293–1300.
19. Zhang, G., Li, C., Li, Q., Li, B., Larkin, D.M., Lee, C., Storz, J.F., Antunes, A., Greenwold, M.J., Meredith, R.W., *et al*.; Avian Genome Consortium (2014). Comparative genomics reveals insights into avian genome evolution and adaptation. Science *346*, 1311–1320.
20. Alex Buerkle, C., and Gompert, Z. (2013). Population genomics based on low coverage sequencing: how low should we go? Mol. Ecol. *22*, 3028–3035.
21. Han, E., Sinsheimer, J.S., and Novembre, J. (2014). Characterizing bias in population genetic inferences from low-coverage sequencing data. Mol. Biol. Evol. *31*, 723–735.
22. Nadachowska-Brzyska, K., Burri, R., Olason, P.I., Kawakami, T., Smeds, L., and Ellegren, H. (2013). Demographic divergence history of pied flycatcher and collared flycatcher inferred from whole-genome re-sequencing data. PLoS Genet. *9*, e1003942.
23. Weber, C.C., Nabholz, B., Romiguier, J., and Ellegren, H. (2014). Kr/Kc but not dN/dS correlates positively with body mass in birds, raising implications for inferring lineage-specific selection. Genome Biol. *15*, 542.
24. Brommer, J.E., Gustafsson, L., Pietiäinen, H., and Merilä, J. (2004). Single-generation estimates of individual fitness as proxies for long-term genetic contribution. Am. Nat. *163*, 505–517.
25. Abouheif, E. (1999). A method for testing the assumption of phylogenetic independence in comparative data. Evol. Ecol. Res. *1*, 895–909.